博　士　論　文

Study of function and formation of a novel mitosis-specific dynamic actin structure in *Dictyostelium* cells

（細胞性粘菌の分裂期特異的な新奇アクチン動的構造の機能と形成の研究）

平成２０年　３月

Go Itoh

（伊藤　剛）

山口大学大学院理工学研究科

Index

Abbreviations used in this paper: GFP, green fluorescent protein; IRM, interference refection microscope; MiDAS, mitosis-specific dynamic actin structure; MHC, myosin heavy chain(s); TIRF, total internal reflection fluorescence

Summary

Cell division of various animal cells depends on their attachment to a substratum. *Dictyostelium* cells deficient in type II myosin, analogous to myosin in muscle, can divide on substratum without the contractile ring. To investigate the mechanism of this substratum-dependent cytokinesis, the dynamics of actin in the ventral cortex was observed by confocal and total internal reflection fluorescence microscopy. Specifically during mitosis, we found novel actin-containing structures (MiDASes: mitosis-specific dynamic actin structures) underneath the nuclei and centrosomes. When the nucleus divided, the MiDAS also split in two and followed the daughter nuclei. At that time, the distal ends of astral microtubules reached mainly the MiDAS regions of the ventral cortex. A microtubule inhibitor induced disappearance of MiDASes leading to the aborted cytokinesis, suggesting that astral microtubules are essential to the formation and maintenance of MiDASes. Fluorescence recovery after photobleaching experiments revealed that the MiDAS was highly dynamic and composed of small actin dot-like structures. Interference reflection microscopy and assays blowing away the cell bodies by jet streaming showed that MiDASes were major attachment sites of dividing cells. Thus, the MiDASes are strong candidates for scaffolds for substratum-dependent cytokinesis transmitting mechanical force to the substratum.

Introduction

Cytokinesis is the final step of mitosis. In most animal cells, a contractile ring, which is mainly composed of actin and myosin, is formed at the cleavage plane and divides a parent cell body into two daughter cells. The contraction of the contractile ring is mediated by the interaction between actin and myosin in a mechanism analogous to the contraction of muscle. In suspension culture, *Dictyostelium* cells become multinucleated and finally lyse when a single copy of the myosin II heavy chain gene is deleted by homologous recombination (DeLozanne and Spudich, 1987) or silenced by antisense RNA (Knecht and Loomis, 1987). However, these myosin null cells can still divide on the substratum.

When multinucleated myosin II null cells in suspension culture are placed on the substratum, they tightly adhere to the substratum and divide without preceding ordinary nuclear division. This phenomenon is called "traction-mediated cytofission", and the traction force against the substratum generated by two daughter cells is considered to mediate this type of cytokinesis (Spudich, 1989; Fukui et al., 1990). Interestingly, when myosin II null cells are cultured on the substratum, they can divide in a cell cycle-dependent manner, via almost morphologically normal cytokinesis (Gerisch and Weber, 2000). This 'cell cycle-dependent' cytokinesis is distinguished from the traction-mediated cytofission and referred to as cytokinesis B (Neujahr et al., 1997; Zang et al., 1997). Uyeda et al. (Uyeda et al., 2000) renamed these three modes of cytokinesis as follows: the myosin II-dependent (contractile ring-dependent) cytokinesis is cytokinesis A, cell cycle-dependent and myosin II-independent cytokinesis is

cytokinesis B, and cell cycle-independent and myosin II-independent cytokinesis is cytokinesis C. The molecular mechanisms of cytokinesis B and C have not been clarified to date. Probably, these types of cytokinesis are mediated by the traction force generated by two daughter cells. Recent research has shown similar substratum-dependent and contractile ring-independent cytokinesis in mammalian cells (Kanda et al., 2005).

Signal pathways for the cytokinesis B remain unknown. Previously, coronin and amiA are identified to contribute to the cytokinesis B (Nagasaki et al, 2002). Myosin II null cells defected in either coronin or amiA gene frequently failed to cytokinesis B and then became gradually multinucleate on substratum, although the disruption of these genes in WT cells had no effect in cytokinesis A. Therefore, cytokinesis B is regulated through a different signal pathway from cytokinesis A.

Several actin-containing structures have been described in *Dictyostelium* cells. Filopods, long thin extensions containing actin-bundles; microvilli, short thin extensions containing actin-bundles; and pseudopods or lamellipods, large extensions containing dense actin-meshworks, are mainly observed at the anterior half of migrating cells and the polar regions of dividing cells (Yumura et al., 1984), which are common to many animal cells. *Dictyostelium* cells have no large actin-bundles inside the cell, such as stress fibers. Actin filaments are mainly localized at the cortex to form an actin cortex. During phagocytosis, the cell forms a phagocytic cup surrounding of the solid food, which is formed by actin-mesh. Crown-like structures (de Hostos et al., 1991) are observed mainly in cells drinking fluid medium, and sometimes behave as pseudopods.

Actin filaments also form clusters at the focal adhesion for cell migration.

In the present study, to investigate the role of actin in substratum-dependent cytokinesis, actin dynamics in myosin II null cells expressing GFP-actin was observed by total internal reflection fluorescence (TIRF) microscopy. We found novel dynamic actin structures, which appeared specifically during mitosis. We referred to these novel structures as MiDASes (M-phase specific dynamic actin structures), and investigated their dynamics and functions. Our results demonstrate that MiDASes are formed beneath the centrosomes by some signals transmitted along astral microtubules and play an important role in cytokinesis as scaffolds for transmitting the traction force to the substratum.

Materials and Methods

Cell culture and transformation

Myosin II heavy chain null cells (HS1) were cultured in a plastic dish at 22°C in HL5 medium (1.3% bacteriological peptone, 0.75% yeast extract, 85.5 mM D-glucose, 3.5 mM Na_2HPO_4 $12H_2O$, 3.5 mM KH_2PO_4, pH 6.5). Plasmid DNA constructs including GFP-actin, mCherry-actin, GFP-α-tubulin and GFP-histone1 were transformed into cells by electroporation (Yumura et al., 1995). Briefly, cells that grew confluently in plastic dish were washed twice with 15 mM Na/K phosphate buffer, and they were centrifuged at 2,000 rpm for 90 seconds at 4°C. After centrifuging, an equal volume of the phosphate buffer was added to the pellet, and then suspended by mild tapping. Thirty micro liters of the cell suspension and 3 μl of plasmid DNA solution were mixed, and charged at 380 V twice. After electroporation, the solution in the cuvette was suspended in 10 ml of HL5 medium including 40 μg / ml of streptomycin in plastic Petri dish. After 12 hours, 10 μg / ml of G418 (Sigma) and / or Blasticidin (Kaken) was added for selection.

Treatment with thiabendazole

Cells expressing GFP-actin or GFP-α-tubulin that grew in HL5 medium were washed with BSS (10 mM $NaCl_2$, 10 mM KCl, 3 mM $CaCl_2$, 2mM MES, pH 6.3). After incubating for 3 hours, cells were placed in a chamber that was made by attaching a silicon sheet with a hole (10 mm in diameter) to a 24 x 50 mm coverslip. An equal amount of thiabendazole (2×10^{-4} M in BSS) was added to the chamber. HS1 cells

took 4-7 min to divide. Microtubules disappeared within about 30 sec as shown in Fig. 4A. Then thiabendazole was removed by replacing with BSS. The cells were observed by confocal microscopy (LSM510, Carl Zeiss).

Fixation and staining

HS1 cells expressing GFP-histone1 or GFP-α-tubulin that grew in HL5 medium were suspended and then placed on 18 x 18 mm coverslip. After 20 minutes, fixation was performed with ethanol containing 1% (w / v) formaldehyde at -17 °C for 5 minutes. After washing 3 times with PBS (135 mM $NaCl_2$, 2.7 mM KCl, 1.5 mM KH_2PO_4, 80 mM NaH_2PO_4, pH 7.3) at 5 minutes intervals, cells were incubated with tetramethyl rhodamine (TRITC)-phalloidin for 30 minutes, and then washing 3 times with PBS with 5 minutes intervals. After mounting the samples in mounting medium [10% polyvinyl alcohol in PBS containing 50% (v / v) glycerol], the cells were observed by confocal microscopy.

Confocal microscopy

Fluorescence images of HS1 cells expressing GFP-actin or GFP-α-tubulin were obtained with confocal microscope system, LSM 510 microscope (Carl Zeiss) equipped with a 100 x Plan Neofluar objective (NA 1.3). For excitation of GFP and TRITC, the argon laser (488 nm line) and HeNe laser (543 nm line) were used respectively. Time-lapse microscopy of HS1 cell expressing GFP-actin was preformed at optical section of 1.6 μm with focusing on the ventral surface of the cell. To acquire

sequential fluorescence images from bottom to top, confocal sections were scanned up at distances of 0.3 μm in the Z-axis. Interference reflection microscopy (IRM) images and fluorescence images were simultaneously performed as described previously (Uchida and Yumura, 2004). Photobleaching was performed as described previously (Yumura, 2001). Measurement of fluorescence intensity was used by Scion software (Scion Corporation). To perform an assay blowing away the cell bodies, the cell bodies were blown away by a jet stream of the buffer from a pipette under confocal microscopy.

Total internal reflection fluorescence (TIRF) microscopy

The TIRF microscopy system (based on I X70, Olympus) was constructed as previously described (Tokunaga et al., 1997). Fluorescence of HS1 cells expressing GFP-actin was observed with the TIRF microscope equipped with PlanApo oil objective (60 X, NA 1.45, Olympus). Illumination was performed by argon laser (40 mW, the National Laser) and HeNe laser (2 mW, Reserch Electro Optics). The fluorescence images were captured by the digital cooled CCD camera (C4742-95-12 ER, Hamamatsu), and digitized with IP lab software for MS Windows (Scanalytics, Inc.).

Results

A novel mitosis-specific dynamic actin structure (MiDAS)

Dictyostelium cells deficient in myosin II can divide on a substratum although they cannot in suspension culture. In order to investigate the mechanism of this substratum-dependent cytokinesis, we observed the dynamics of actin in the ventral cortex of dividing myosin II null cells expressing GFP-actin on the substratum by total internal reflection fluorescence (TIRF) microscopy, which illuminates only about 100 nm above the coverslip. Consistent with the observation by conventional fluorescence microscopy (Yumura et al., 1984), actin localized to polar pseudopods of dividing cells (arrowheads in Fig. 1A). TIRF microscopy revealed other major structures containing actin (circles in Fig. 1A), which were not observed in interphase cells (Fig. 1B) but only in the mitotic cells. Therefore, these structures are referred to as MiDAS (mitosis-specific dynamic actin structure) hereafter. A MiDAS emerged as an irregularly shaped and large flat sheet in the middle of the ventral cell cortex when the spindle began to elongate. The MiDAS split in two in accord with the nuclear division and moved to each daughter cell. The MiDASes dynamically changed their shape and size from 2-5 μm in diameter. The trajectories of two MiDASes during cell division are shown in Fig. 1C. Fig. 1D shows the time course of the area of MiDASes, showing that they disappeared shortly after the completion of cytokinesis. When the cells were treated with latrunculin A, a depolymerizer for actin filaments, MiDASes disappeared within about 40 sec (data not shown). In addition, MiDASes were stained with tetramethyl rhodamine-phalloidin as shown in the next section. Therefore,

MiDASes are composed of actin filaments. MiDASes were also observed in dividing wild type cells although the appearance was very transient (Fig. 1E). Thus the MiDAS is a novel mitosis-specific actin-containing structure as far as we know.

Astral microtubules are required for the formation and maintenance of MiDASes.

Fig. 2A-F shows a series of optical sections by confocal microscopy of fixed multinucleated cells expressing GFP-histone1, which shows the position of nuclei, and stained with tetramethyl rhodamine-phalloidin, which is specifically bound to actin filaments. Multinucleated cells were prepared in suspension culture since myosin null cells cannot divide in suspension. Fig. 2H-M shows multinucleated cells expressing GFP-α-tubulin stained with tetramethyl rhodamine-phalloidin. MiDASes are located underneath the nuclei and the centrosomes. The latter two organelles were associated with each other. The number of MiDASes was consistent with that of nuclei and centrosomes. These observations suggest the possibility that nuclei and/or centrosomes may induce the formation of MiDASes. Centrosomes especially are more plausible because astral microtubules emerging from them can directly reach the ventral cortex to induce formation of MiDASes.

To assess this possibility, MiDASes and microtubules were simultaneously observed in live cells expressing mCherry-actin and GFP-α-tubulin by confocal microscopy (Fig. 3A-C). Consistent with the observation of fixed cells, MiDASes were located underneath the centrosomes and, interestingly, relocated following the movement of centrosomes (Fig. 3B,C). Since TIRF microscopy can limit illumination to about 100

nm above the coverslip, which corresponds to the thickness of the ventral cortex including actin cortex and MiDASes, it is possible to observe the correlation between the distal ends of each microtubule and the MiDASes. Fig. 3D shows typical images of the relationship between the distal ends of microtubules and MiDASes which were captured by 100 milliseconds-exposure. Fig. 3E shows a sum of traces of microtubules (green) and outlines of MiDAS (red) for 15 seconds, indicating that the distal ends of microtubules reached mainly in the MiDAS regions. These observations strongly suggest that astral microtubules emerging from the centrosomes determine the position of MiDASes, probably by sending signals to the ventral cortex.

To further examine the possible role of microtubules in the formation of MiDASes, myosin null cells were exposed to thiabendazole, which specifically disrupts microtubules, in a similar way to nocodazole (Kitanishi et al., 1984). Shortly after the addition of thiabendazole, astral microtubules shortened (Fig. 4A), and MiDASes gradually regressed in size and finally disappeared (Fig. 4B). When thiabendazole was removed by washing with buffer, MiDASes appeared underneath the centrosomes again (arrows in Fig. 4B). These results strongly suggest that the astral microtubules carry some signals to the cortex, which are involved in the formation and maintenance of MiDASes.

MiDASes are required for substratum-dependent cytokinesis

Myosin null cells fail to complete cytokinesis on substratum with a frequency of about 10% (Neujahr et al., 1997). In such cases, half of the dividing cells was resorbed by

the other half, probably due to an imbalance in the motile activities between the two halves. We frequently observed abortive cytokinesis when MiDASes disappeared by accident. When one of the MiDASes disappeared (arrows in Fig. 5A), this half of the cell was finally resorbed by the other. Quantitative analysis shows that the area of MiDAS decreased coincidentally with that of the resorbed half (Fig. 5B).

To assess the role of MiDASes in completion of cytokinesis, MiDASes were artificially disrupted by treatment with thiabendazole, a microtubule inhibitor. All of the cells in the early stage of cytokinesis (n=26) that lost MiDASes after the treatment with thiabendazole failed in cytokinesis (Fig. 5C). These observations indicate that the MiDAS is required for cytokinesis of myosin null cells, or substratum-dependent cytokinesis.

MiDAS function as scaffolds for substratum-dependent cytokinesis

Since MiDASes exist in the ventral cell cortex and are necessary for substratum-dependent cytokinesis, they may transmit the traction force generated by the cell to the substratum. If this is the case, the cell membrane underneath MiDASes must be attached to the substratum. To assess this possibility, myosin null cells were observed by interference reflection microscopy (IRM), which is generally used to detect adhesion sites of cells. Fig. 6A shows dual images of GFP-actin and IRM, which shows the existence of darker tone at the MiDAS regions than the other ventral membrane, suggesting that MiDAS regions are closer to the substratum than the other regions of the ventral membrane.

To further assess whether the dividing cells attached to the substratum at the MiDAS regions, cell bodies were blown away by a jet stream of buffer from a pipette under confocal microscopy. Fig. 6B and C show MiDASes before and after blowing away the cell bodies. In many cases, only MiDAS regions remained attached to the substratum although other parts of the cells were detached by the blowing, indicating that dividing cells strongly attached to the substratum mainly at the MiDAS regions.

These observations strongly suggest that MiDASes are scaffolds for substratum-dependent cytokinesis and platforms for the cell to transmit mechanical force to the substratum.

Dynamics of actin in MiDAS

The size and shape of MiDASes were not constant but changed dynamically. To investigate dynamics of actin in MiDASes, a part of the MiDAS region was photobleached by scanning laser illumination. The fluorescence of the bleached regions immediately recovered (Fig. 7A and B, half time of the recovery, 2.15 ± 0.89 seconds, mean $\pm$ s.d., n= 17), which indicates that actin in the MiDASes undergoes continuous rapid turnover. Fig. 7C and D show high magnifications of the fluorescence recovery processes. After photobleaching, fluorescence appeared as individual small dots and finally became an aggregate of these dots.

Next, we examined how MiDASes first emerged in the early anaphase and how they disappeared after the completion of cytokinesis. Nascent MiDASes were composed of multiple small actin dots. Importantly, these small actin dots did not change their

position; they appeared and then disappeared at the same position (arrows in Fig. 8A). The average duration of the appearance was 18.17 ± 3.13 seconds (n = 400 dots, 10 cells). The dots gradually increased in number and they fused with each other to become a large MiDAS. Likewise, after the final stage of cytokinesis, small actin dots in MiDASes gradually disappeared and the size of MiDAS gradually decreased (Fig. 8B). These small actin dots seemed to be identical to 'actin foci', which are considered as focal adhesions for migration of *Dictyostelium* cells (Yumura and Kitanishi-Yumura, 1990; Uchida and Yumura, 2004). Actin foci also appeared and disappeared with a duration similar to actin dots in MiDASes. However, since actin foci still exist even after the disappearance of MiDASes induced by the disruption of microtubules, the formation of actin foci does not seem to be regulated by microtubules (Fig. 5C).

These observations suggest that the MiDASes are composed of small actin dots, which rapidly turn over, and the MiDASes can change their location as a whole via this dynamic turnover.

Discussion

In *Dictyostelium* cells, myosin II null cells can still divide on substratum, though they will die in suspension culture. It has been considered that the substratum-dependent cell division progresses through the traction force generated as the splitting daughter halves migrate in opposite directions. We investigated the role of actin in this substratum-dependent and myosin II-independent cytokinesis. Careful observation of myosin II null cells expressing GFP-actin by TIRF microscopy allowed us to find novel actin structures (MiDASes), which appear specifically during mitosis. MiDASes emerged underneath the centrosomes, split in two, and moved following the centrosomes. The distal ends of astral microtubules emerging from the centrosomes reached mainly the MiDAS regions. When MiDASes disappeared accidentally or artificially by microtubule inhibitors, cells showed abortive cytokinesis, regardless of protrusion of pseudopods at the both poles (Fig. 5A, C). In addition, the cell membrane at the MiDAS regions was tightly attached to the substratum, and disappearance of MiDAS highly induced a resorbing of daughter cell (Fig. 5A, B). Accordingly, MiDASes may function as wedges for overcoming the detachment from substratum due to uneven traction force of both daughter halves. Thus, MiDASes can play an important role as scaffolds for the substratum-dependent cytokinesis.

Because astral microtubules were indispensable for the formation of MiDASes, there may be some signals along the astral microtubules that induce the formation and maintenance of MiDASes. Our observation by TIRF microscope showed that only a few microtubules touched to the ventral cortex underneath MiDAS. In addition, the

area of MiDAS was much wider than that of the attached microtubules. Diffusive signal mediated microtubules may require for an initiation the formation or maintain of MiDAS. In vertebrate animal cells, CLIP 170, EB1, and APC (collectively termed '+Tips'), which associate to the plus ends of microtubules, regulate actin cytoskeleton at the leading edges (Fukata et al., 2002; Kawasaki et al., 2000; Wen et al., 2004). EB1 has been identified also in *Dictyostelium* cells, and colocalizes with actin (Rehberg and Graf, 2002), but whether DdEB1 induces the expansion of pseudopods is still unknown. In the case of 3T3 fibroblasts, the ruffling is induced by Rac 1, one of small G proteins, which is activated by polymerizing microtubules (Waterman-Storer et al., 1999). Since the plus ends of astral microtubules are concentrated at the polar regions of a dividing cell, they may activate ruffling there (Neujahr et al., 1998). In our observations, MiDASes sometimes fused with actin of pseudopods (data not shown), suggesting that similar signals by plus ends of astral microtubules may induce actin polymerization both in pseudopods at the leading edges and MiDASes in the ventral cell cortex.

As shown in Fig. 8A, small actin dots increased in number and formed a nascent MiDAS in the early anaphase. Inversely, when MiDASes disappeared after the completion of cytokinesis, actin dots decreased in number (Fig. 8B). These observations suggest that MiDASes are composed of actin dots. Interestingly, the individual actin dots did not change their positions; they appeared and disappeared at the same positions. These actin dots were indistinguishable from actin foci; the duration of their appearance and their sizes were identical. Our previous study has

shown that actin foci are fixed in position relative to the substratum and are a candidate for feet of *Dictyostelium* during cell migration (Uchida and Yumura, 2004). Apparently MiDASes changed their position so as to coordinate with the position of the centrosomes (Fig. 1 and 3). The change in the position of MiDASes can be explained by this rapid turnover of actin dots; their appearance in the front leading edge of the MiDAS and their disappearance in the rear result in a gradual change in the location of the MiDAS as a whole. Recent TIRF microscopy revealed mobile actin clusters, the size of which were similar to actin foci, during the reorganization of actin networks after they were depolymerized by latrunculin A and then the drug was removed (Gerisch et al., 2004). The actin foci and the actin dots in the MiDAS seem to be different from the actin clusters because the former are stationary with respect to the substratum.

Do wild type *Dictyostelium* cells perform cytokinesis by dual mechanisms, myosin II-dependent and -independent mechanisms? MiDASes appear transiently even in wild type cells (Fig. 1E). When wild type cells divide on substratum, most of them round up, suggesting that most of contact sites are detached from the substratum. However, some of the population divides with adhering strongly to the substratum, keeping their flat morphology. In this case, the cellular shape during mitosis is similar to that of myosin II null cells (Neujahr et al., 1997; Nagasaki et al., 2001). Probably, wild type cells divide through both myosin II-dependent and -independent mechanisms. It is also plausible that the appearance of MiDAS may be a result of adaptation in myosin null cells, which is transitory and less important in wild type cells because they can divide without substratum. Myosin II-independent cell division has also been

observed in mammalian cells. Epitheloid kidney cells injected with anti-myosin antibodies to diminish levels of myosin II in the equatorial region could still divide (Zurek B et al., 1990). Normal rat kidney cells can divide in the presence of blebbistatin, a myosin II inhibitor, in a similar manner to *Dictyostelium* myosin null cells (Kanada et al., 2005). Normal kidney cells and 3T3 fibroblasts that were microinjected with C3 ribosyltransferase, an inhibitor of Rho, could not accumulate myosin at the cleavage furrow but still divided (O'Connell et al., 1999). This cleavage is considered cell-substratum dependent, because Hela cells, which detach from the substratum during cell division, cannot divide when injected with C3 enzyme. The same authors described that when fluorescent beads were attached to the surface of C3-injected normal rat kidney cells, they moved toward the chromosomes and the resultant cluster of beads followed the movement of chromosomes and split in two as if they were tethered to the chromosomes. At that time, clusters of cortical F-actin were localized under the chromosomes, which is reminiscent of MiDASes (O'Connell et al., 1999). More recently, Guha et al. (Guha et al., 2005) showed that a large actin structure similar to MiDASes appeared in dividing normal rat kidney cells after local treatment with blebbistatin, a potent inhibitor of the nonmuscle myosin II ATPase. It is worth noting that MiDASes can be observed even in myosin null *Dictyostelium* cells expressing motorless myosin II (Itoh and Yumura, unpublished). Therefore, loss of myosin ATPase activities seems to induce the emergence of MiDASes.

Myosin II-independent and adhesion-dependent cell division is probably an ancient mechanism from before the evolution of myosin and still now has been reserved in

various cells (Uyeda et al., 2004). Therefore, the investigation of this mechanism is significant for total understanding of the mechanism of cytokinesis. In future studies, it is important to clarify the putative signals transmitted along the astral microtubules which regulate the formation and maintenance of MiDASes.

References

De Hostos, E. L., Bradtke, B., Lottspeich, F., Guggenheim, R. and Gerisch G. (1991). Coronin, an actin binding protein of *Dictyostelium discoideum* localized to cell surface projections, has sequence similarities to G protein β subunits. *EMBO. J.* **10,** 4097-4104.

De Lozanne, A. and Spudich, J. A. (1987). Disruption of the *Dictyostelium* myosin heavy chain gene by homologous recombination. *Science.* **236,** 1086-1091.

Fukata, M., Watanabe, T., Noritake, J., Nakagawa, M., Yamaga, M., Kuroda, S., Matsuura, Y., Iwamatsu, A., Perez, F. and Kaibuchi, K. (2002). Rac1 and Cdc42 capture microtubules through IQGAP1 and CLIP-170. *Cell.* **109,** 873-885.

Fukui, Y., De Lozanne, A. and Spudich, J. A. (1990). Structure and function of the cytoskeleton of a *Dictyostelium* myosin-defective mutant. *J. Cell Biol.* **110,** 367-378.

Gerisch, G., Bretschneider, T., Muller-Taubenberger, A., Simmeth E., Ecke, M., Diez, S. and Anderson, K. (2004). Mobile actin clusters and traveling waves in cells recovering from actin depolymerization. *Biophys. J.* **87,** 3493-3503.

Gerisch, G. and Weber, I. (2000). Cytokinesis without myosin II. *Curr. Opin. Cell Biol.* **12,** 126-132.

Guha, M., Zhou, M. and Wang, Y. L. (2005). Cortical actin turnover during cytokinesis requires myosin II. *Curr. Biol.* **15,** 732-736.

Kanada, M., Nagasaki, A. and Uyeda, T. Q. P. (2005). Adhesion-dependent and contractile-ring-independent equatorial furrowing during cytokinesis in mammalian cells. *Mol. Biol. Cell.* **16,** 3865-3872.

Kawasaki, Y., Senda, T., Ishidate, T., Koyama, R., Morishita, T., Iwayama, Y., Higuchi, O. and Akiyama, T. (2000). Asef, a link between the tumor suppressor APC and G-protein signaling. *Science.* **289,** 1194-1197.

Kitanishi, T., Shibaoka, H. and Fukui, Y. (1984). Disruption of microtubules and retardation of development of *Dictyostelium* with ethyl N-phenylcarbamate and thiabendazole. *Protoplasma.* **120,** 185-196.

Knecht, D. A. and Loomis, W. F. (1987). Antisense RNA inactivation of myosin heavy chain gene expression in *Dictyostelium discoideum*. *Science.* **236,** 1081-1086.

Nagasaki, A., Hibi, M., Asano, Y. and Uyeda, T. Q. P. (2001). Genetic approaches to dissect the mechanisms of two distinct pathways of cell cycle-coupled cytokinesis in *Dictyostelium*. *Cell Struct. Funct.* **26,** 585-591.

Nagasaki A, De Hostos, E. L. and Uyeda, T. Q. P (2002). Genetic and morphological evidence for two parallel pathways of cell-cycle-coupled cytokinesis in *Dictyostelium*. *J. Cell Sci.* **115**, 2241-2251.

Neujahr, R., Albrecht, R., Kohler, J., Matzner, M., Schwartz, J. M., Westphal, M. and Gerisch, G. (1998). Microtubule-mediated centrosome motility and the positioning of cleavage furrows in multinucleate myosin II-null cells. *J. Cell Sci.* **111,** 1227-1240.

Neujahr, R., Heizer, C. and Gerisch, G. (1997). Myosin II-independent processes in mitotic cells of *Dictyostelium discoideum*: redistribution of the nuclei, re-arrangement of the actin system and formation of the cleavage furrow. *J. Cell Sci.* **110,** 123-137.

O'Connell, C. B., Wheatley, S. P., Ahmed, S. and Wang, Y. L. (1999). The small GTP- binding protein Rho regulates cortical activities in cultured cells during division. *J.*

Cell Biol. **144,** 305-313.

Rehberg, M. and Graf, R. (2002). *Dictyostelium* EB1 is a genuine centrosomal component required for proper spindle formation. *Mol. Biol. Cell.* **13,** 2301-2310.

Spudich, J. A. (1989). In pursuit of myosin function. *Cell Regul.* **1,** 1-11.

Tokunaga, M., Kitamura, K., Saito, K., Hikikoshi-Iwane, A. and Yanagida, T. (1997). Single molecule imaging of fluorophores and enzymatic reactions achieved by objective-type total internal reflection fluorescence microscopy. *Biochem. Biophys. Res. Commun.* **235,** 47-53.

Uchida, K. S. K. and Yumura, S. (2004). Dynamics of novel feet of *Dictyostelium* cells during migration. *J. Cell Sci.* **117,** 1443-1455.

Uyeda, T. Q. P., Kitayama, C. and Yumura, S. (2000). Myosin II-independent cytokinesis in *Dictyostelium*: its mechanism and implications. *Cell Struct. Funct.* **25,** 1-10.

Uyeda, T. Q. P. and Nagasaki, A. (2004). Variations on a theme: the many modes of cytokinesis. *Curr. Opin. Cell Biol.* **16,** 55-60.

Waterman-Storer, C. M., Worthylake, R. A., Liu, B. P., Burridge, K. and Salmon, E. D. (1999). Microtubule growth activates Rac1 to promote lamellipodial protrusion in fibroblasts. *Nat. Cell Biol.* **1,** 45-50.

Wen, Y., Eng. C. H., Schmoranzer, J., Cabrera-Poch, N., Morris, E. J. S., Chen, M., Wallar, B. J., Alberts, A. S., and Gundersen, G. G. (2004). EB1 and APC bind to mDia to stabilize microtubules downstream of Rho and promote cell migration. *Nat. Cell Biol.* **6,** 820-830.

Yumura, S., Mori, H. and Fukui, Y. (1984). Localization of actin and myosin for the study of ameboid movement in *Dictyostelium* using improved immunofluorescence. *J. Cell Biol.* **99,** 894-899.

Yumura, S. and Kitanishi-Yumura, T. (1990). Fluorescence-mediated visualization of actin and myosin filaments in the contractile membrane-cytoskeleton complex of *Dictyostelium discoideum*. *Cell Struct. Funct.* **15,** 355-364.

Yumura, S., Matsuzaki, R. and Kitanishi-Yumura, T. (1995). Introduction of macromolecules into living *Dictyostelium* cells by electroporation. *Cell Struct. Funct.* **20,** 185-190.

Yumura, S. (2001). Myosin II dynamics and cortical flow during contractile ring formation in *Dictyostelium* cells. *J. Cell Biol.* **154,** 137-145.

Zang, J. H., Cavet, G., Sabry, J. H., Wagner, P., Moores, S. L. and Spudich, J. A. (1997). On the role of myosin-II in cytokinesis: division of *Dictyostelium* cells under adhesive and nonadhesive conditions. *Mol. Biol. Cell.* **8,** 2617-2629.

Zurek, B., Sanger, J. M., Sanger, J. W. and Jockusch, B. M. (1990). Differential effects of myosin-antibody complexes on contractile rings and circumferential belts in epitheloid cells. *J. Cell Sci.* **97,** 297-306.

Acknowledgements

I would like to express my deepest thanks to Dr. S. Yumura for constant guiding during the course of this work. I am grateful to Dr. T. Q. P. Uyeda, and Dr. A. Nagasaki (National Institute for Advanced Interdisciplinary Research, and Mechanical Engineering Laboratory) for providing constructs of GFP-α-tubulin, GFP -histone1 and mCherry-actin. I also thanks to Dr. T. Kitanishi-Yumura for helpful discussion. I also thanks to Dr. Y. Iwadate and all members of the Yumura laboratory for the support in progression of this work.

Figures and figure legends

Fig. 1. Dynamics of actin in myosin null (HS1) cells during cell division and interphase. HS1 cells expressing GFP-actin were observed during cell division (A) and interphase (B) by TIRF microscopy. During cell division, actin mainly localized at both polar pseudopods (arrowheads) and at the centers of each daughter cell (circles) (A). The latter structures are referred to as MiDASes in the present study. In interphase, actin mainly localized in pseudopods (arrowheads) at the leading edge of a migrating cell, but any large actin-containing structures such as MiDASes could not be observed (B). Panel (C) shows trajectories of centroids of two MiDASes until the completion of cytokinesis. Arrowhead indicates original position and arrows indicate final positions of each MiDAS. Panel (D) shows the time course of the area of MiDASes in both daughter halves. The arrow shows the timing of complete scission of the cell (410 seconds), showing that they disappeared shortly after the completion of cytokinesis. Bars, 10 μm.

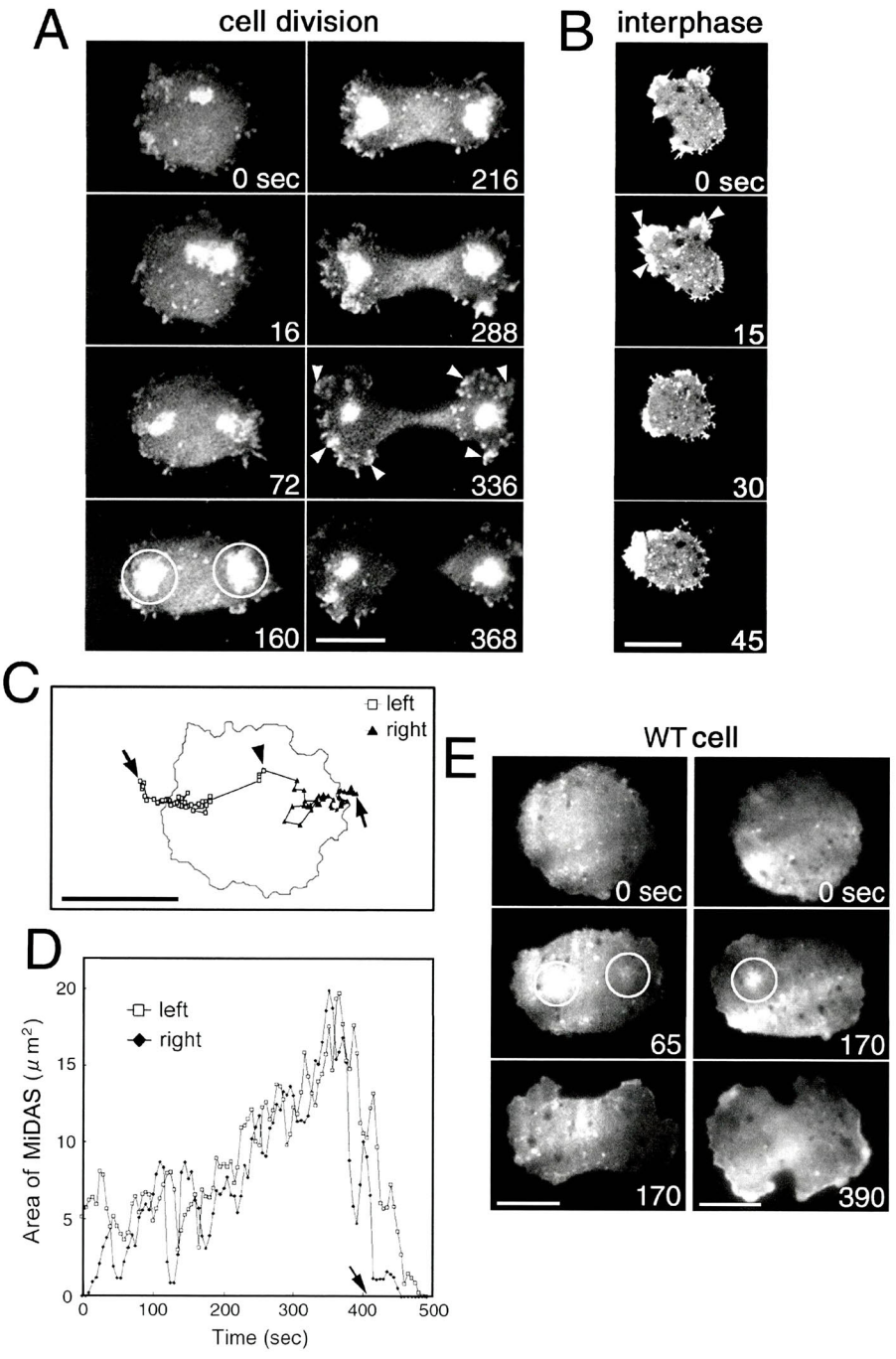
A
cell division
0 sec
216
16
288
72
336
160
368
B
interphase
0 sec
15
30
45
C
left
right
D
left
right
Area of MiDAS (μm^2)
0
5
10
15
20
0
100
200
300
400
500
Time (sec)
E
WT cell
0 sec
0 sec
65
170
170
390

Fig. 2. Distribution of MiDASes, nuclei and centrosomes in multinucleated HS1 cells.

Series of vertical optical sections of a representative multinucleated HS1 cell during cell division. To visualize F-actin and nuclei (A-G), HS1 cells expressing GFP-histone1 (green), which represents the position of nuclei, were fixed and stained with tetramethyl rhodamine-phalloidin (red). Panels (H-N) show the distribution of F-actin (red) and GFP-α-tubulin (green). The optical sections are 1.5 μm in thickness and apart each other by 0.6 μm (A-F and H-M). Panels (G and N) show 3D-reconstructed images from panels (A-F and H-M), respectively. The positions of MiDASes (arrows) correspond to those of nuclei and centrosomes, respectively. Bars, 10 μm.

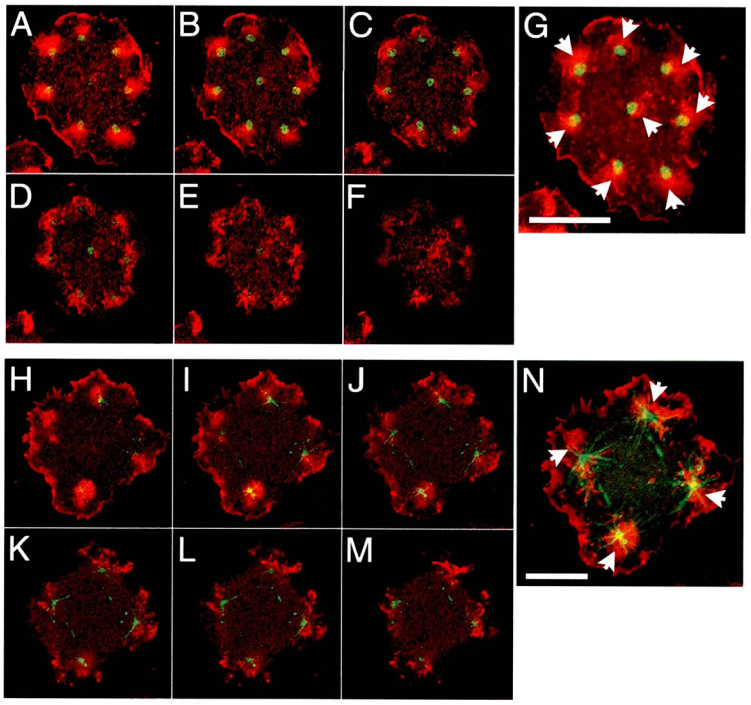
A
B
C
G
D
E
F
H
I
J
N
K
L
M

Fig. 3. Centrosomes and astral microtubules determine the position of MiDASes. MiDASes and centrosomes were simultaneously observed in live HS1 cells expressing mCherry-actin and GFP-α-tubulin (A). Panels (B) show sequential images in the box of panels A. The centroid of MiDAS (closed circle) relocated following the movement of centrosome (open circles). Panel (C) shows trajectories of a centrosome (green line) and a MiDAS (red line) for 99.9 seconds, respectively. Arrowheads indicate original positions and black arrows indicate final positions of the centrosome and the MiDAS, respectively. Panels (D) show TIRF microscopy of a typical dividing multinucleated cell having 4 MiDASes, showing the distal ends of microtubules (green) in the MiDAS regions (arrows). These images were captured by 100 mseconds-exposure. Panel (E) shows a sum of traces of microtubules (green) and outlines of MiDASes (red) for 15 seconds, indicating that the distal ends of microtubules reaching to the ventral cell cortex are mainly limited to MiDAS regions. Bars, 2 μm.

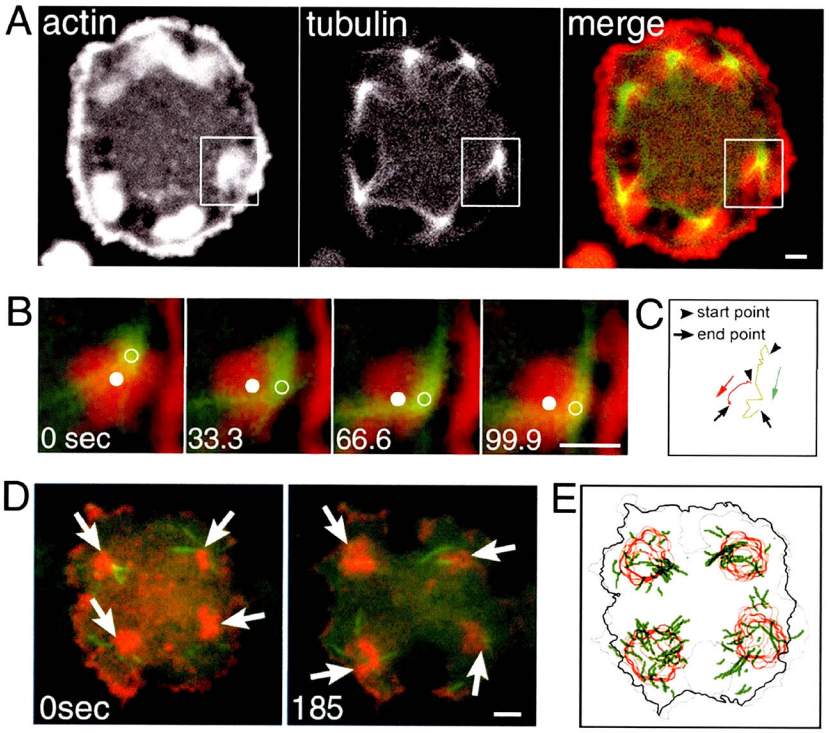
A
actin
tubulin
merge
B
0 sec
33.3
66.6
99.9
C
start point
end point
D
0sec
185
E

Fig. 4. Astral microtubules are required for the formation and maintenance of MiDASes. HS1 cells expressing GFP-α-tubulin (A) or GFP-actin (B) were exposed to thiabendazole, an inhibitor of microtubules, under confocal microscopy. Shortly after the addition of thiabendazole, astral microtubules shortened (A), and MiDASes (arrowheads in B) gradually regressed in size and finally disappeared (0-65 seconds in panels B). When thiabendazole was removed by washing with buffer 65 seconds after addition of thiabendazole, MiDASes gradually appeared underneath the centrosomes again (105-160 seconds). The arrows indicate reappeared MiDASes (160 seconds). Bars, 5 μm.

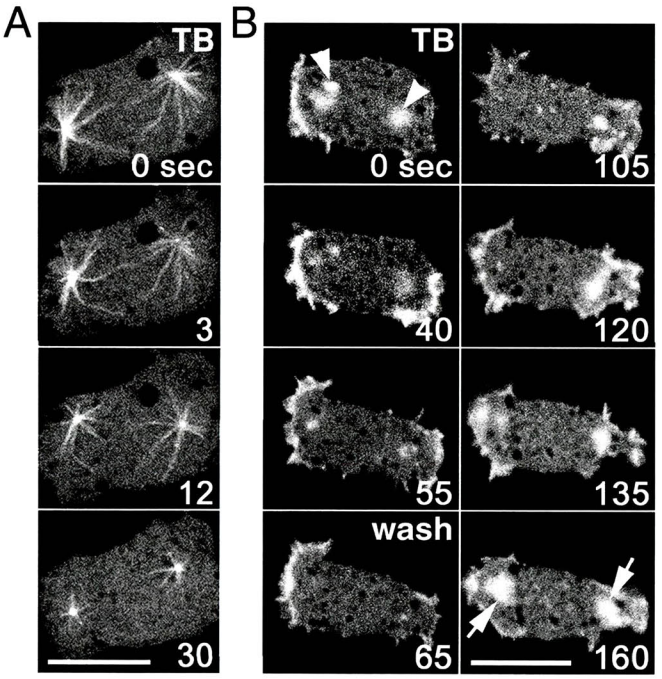
A
TB
0 sec
3
12
30
B
TB
0 sec
105
40
120
55
135
wash
65
160

Fig. 5. Loss of MiDASes results in the failure of cytokinesis.

Dividing HS1 cells expressing GFP-actin were observed by confocal microscopy. When one of the MiDASes (arrows) disappeared by accident, the other half of the cell resorbed this half and eventually the cell failed to complete cytokinesis (A). The arrows indicate the position of the MiDAS in the resorbed half of the cell. Panel (B) shows time course of area of left (closed rectangle) and right (closed triangle) halves, which are divided by a line in panel A. Note that the area of resorbing half (open arrowhead) rapidly decreased after the disappearance of MiDAS (closed arrowhead). Also when the disappearance of MiDASes was artificially induced by the treatment with thiabendazole, all of the cells (n=26 cells) failed to divide (C). Bars, 10 μm

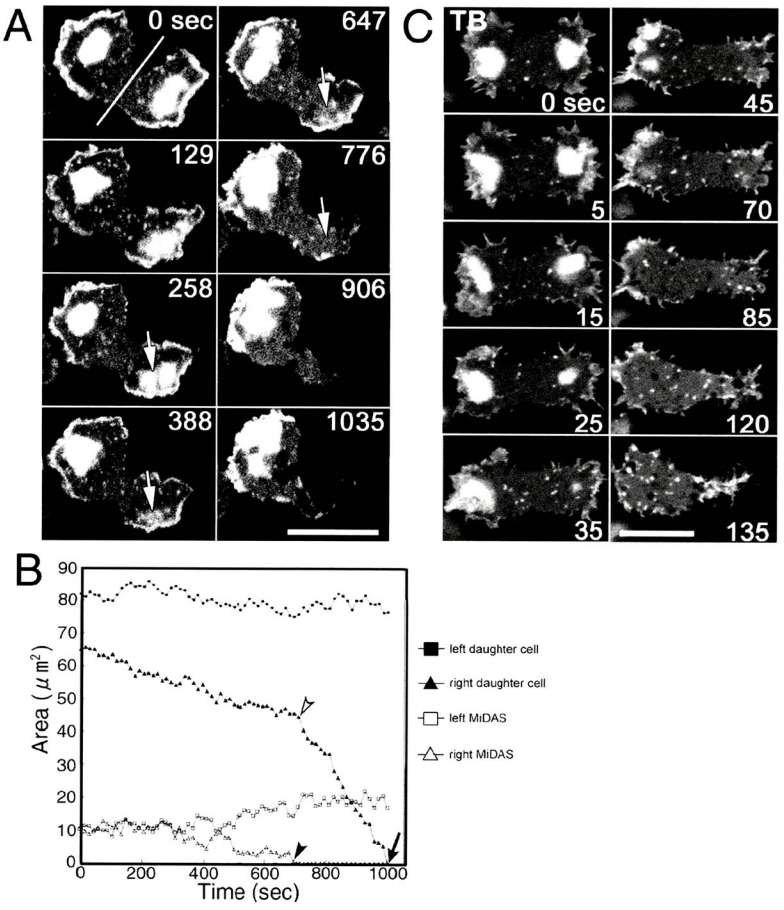
A
0 sec
647
129
776
258
906
388
1035
C
TB
0 sec
45
5
70
15
85
25
120
35
135
B
Area (μm^2)
Time (sec)
left daughter cell
right daughter cell
left MiDAS
right MiDAS

Fig. 6. Dividing cells attach to the substratum at MiDAS regions.

A representative dividing multinucleated HS1 cell was observed by fluorescence microscopy and interference reflection microscopy (IRM). Left panels show fluorescence images of GFP-actin and right panels show IRM images, respectively. (A) IRM images represent darker tone (arrowheads) at MiDAS regions than other ventral membrane. Therefore, cell membrane at MiDAS regions is closer to the substratum than the other ventral cell membrane. In panels (B and C), cell bodies were blown away by a jet stream of buffer from a pipette under confocal microscopy. Right panels show a half of dividing cells before blowing, and left panels show the same areas after blowing away the cell bodies by fluorescence microscopy for GFP actin and phase contrast microscopy. The figures are representative results from 20 cells. Note that only MiDAS regions remained to attach to the substratum, indicating that dividing cell strongly attached to the substratum mainly at the MiDAS regions. Bar, 5 μm.

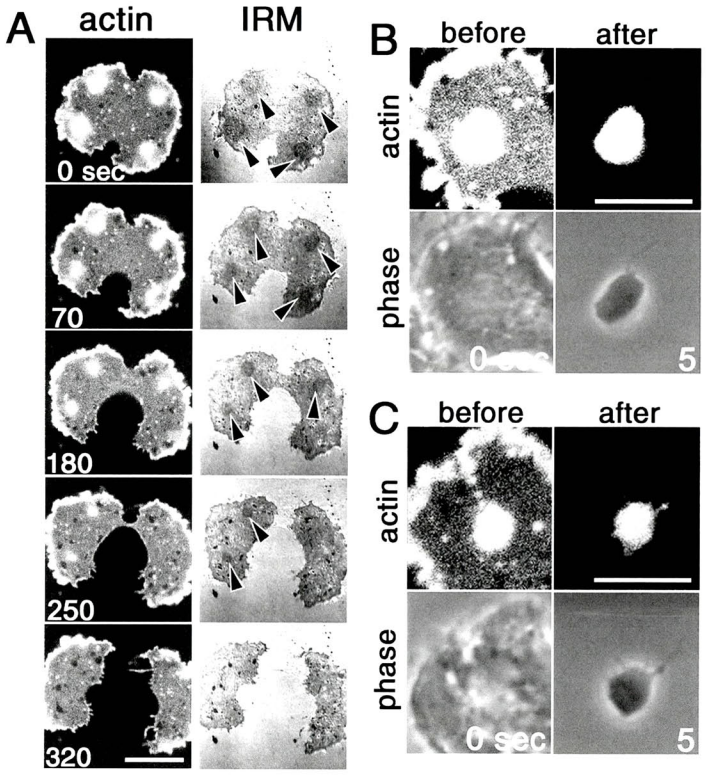
A
actin
IRM
0 sec
70
180
250
320
B
before
after
actin
phase
0 sec
5
C
before
after
actin
phase
0 sec
5

Fig. 7. Actin rapidly turns over in MiDASes.

Fluorescence of a part of MiDAS regions (within black squares) was bleached in HS1 cells expressing GFP-actin (A). The fluorescence of the bleached region shortly recovered after photobleaching (B). The half time of recovery was 2.15 ± 0.89 seconds (mean ± s.d., n = 17). Panels (C and D) show a high magnification of the fluorescence recovery experiments. After photobleaching, fluorescence appeared as individual small fluorescent dots (arrowheads) and finally formed an aggregate. Panel (D) shows images inside the square in panel (C). Bar, 2 μm.

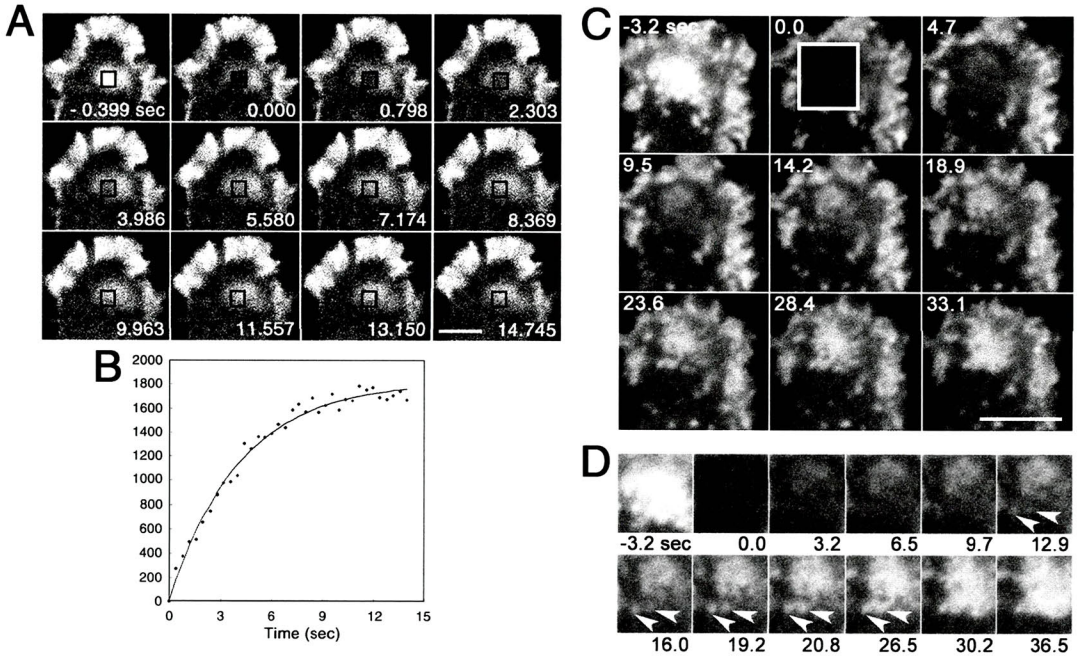
A
- 0.399 sec
0.000
0.798
2.303
3.986
5.580
7.174
8.369
9.963
11.557
13.150
14.745
B
2000
1800
1600
1400
1200
1000
800
600
400
200
0
0
3
6
9
12
15
Time (sec)
C
-3.2 sec
0.0
4.7
9.5
14.2
18.9
23.6
28.4
33.1
D
-3.2 sec
0.0
3.2
6.5
9.7
12.9
16.0
19.2
20.8
26.5
30.2
36.5

Fig. 8. MiDASes are composed of 'dots' of actin.

HS1 cells expressing GFP-actin were observed by TIRF microscopy. In the early stage of mitosis, a nascent MiDAS (arrowhead) was formed by aggregation of many small actin dots (A). These small actin dots did not change their positions; they appeared and then disappeared at the same position (panels A, arrows). On the other hand, during the final stage of cytokinesis these actin dots in MiDASes gradually disappeared and the size of the MiDAS gradually decreased (B). Bar, 2 μm.

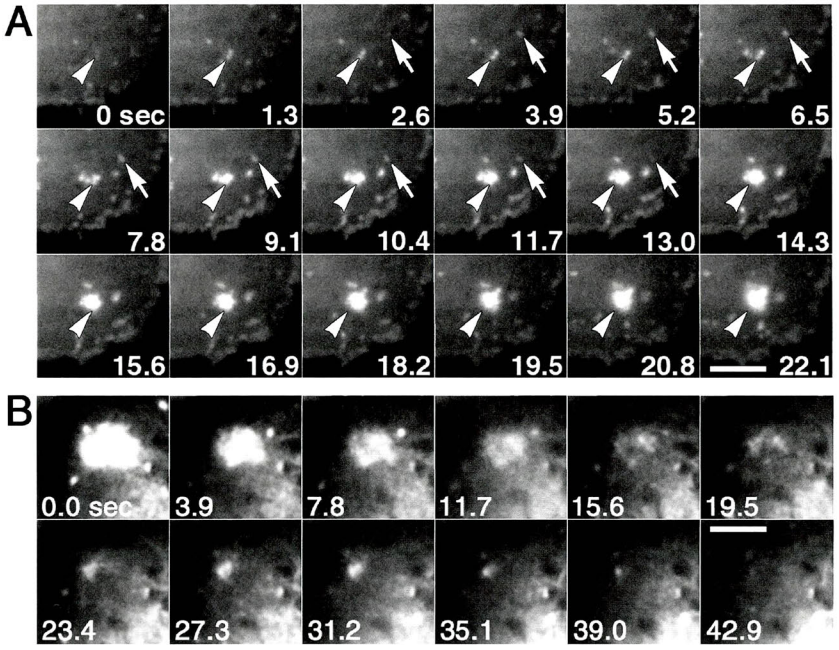
A
0 sec
1.3
2.6
3.9
5.2
6.5
7.8
9.1
10.4
11.7
13.0
14.3
15.6
16.9
18.2
19.5
20.8
22.1
B
0.0 sec
3.9
7.8
11.7
15.6
19.5
23.4
27.3
31.2
35.1
39.0
42.9

Legend for Supplemental Fig. 1 (Fig. S1)

Alternation of area of MiDAS.

The area of MiDASes alternated in each daughter half with a period of about 24.2 ± 5.3 sec (n=10, A). Two sequential images are shown in white boxes in A (B). Graph C shows alternation of the area of MiDAS in left and right half. The white and black arrowheads show the peaks of the area in each MiDAS. This phenomenon occurred in about 20% of the examined cells (44 cells). Bar, 10 μm.

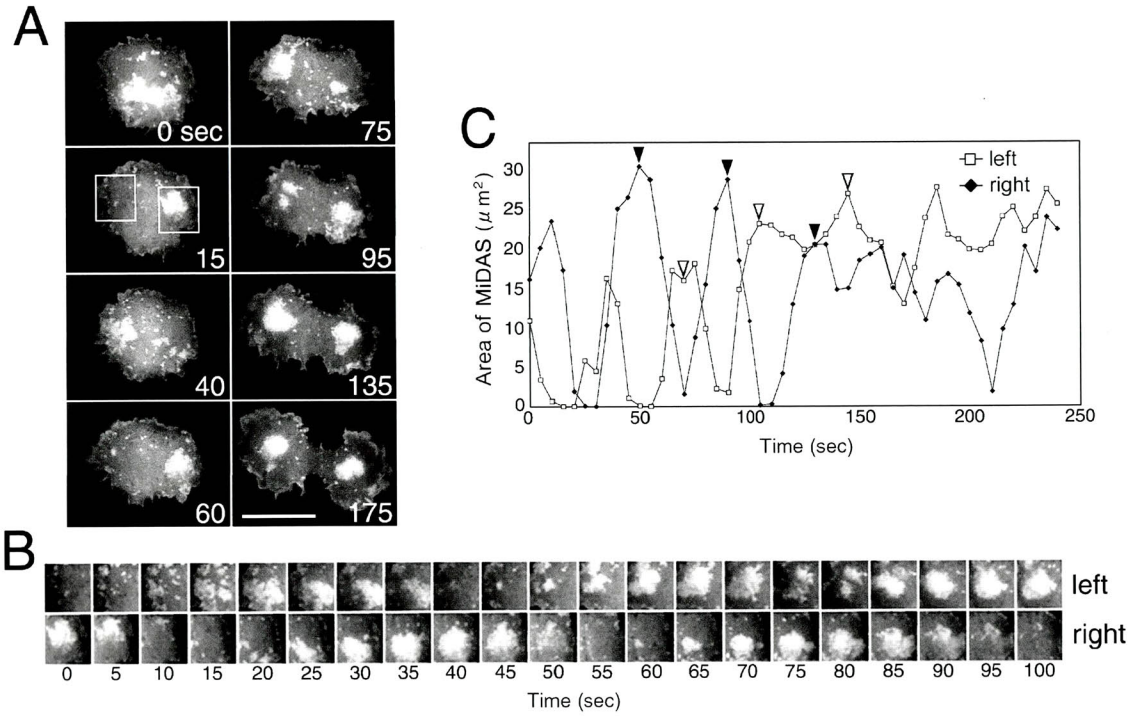
A
0 sec
75
15
95
40
135
60
175
C
left
right
Area of MiDAS (μm^2)
0
5
10
15
20
25
30
0
50
100
150
200
250
Time (sec)
B
left
right
0
5
10
15
20
25
30
35
40
45
50
55
60
65
70
75
80
85
90
95
100
Time (sec)

学位論文の要旨（日本語）

細胞性粘菌の分裂期特異的な新奇アクチン動的構造の機能と形成の研究

(Study of function and formation of a novel mitosis-specific dynamic actin structure in *Dictyostelium* cells)

伊藤　剛

細胞分裂は、核分裂とそれに引き続き起る細胞質分裂によりなる。動物細胞の細胞質分裂は、細胞分裂面に形成される収縮環の収縮により起ると考えられてきた。収縮環の収縮はアクチンとミオシンII（以降ミオシン）の相互作用によって生じる。しかし、近年、収縮環非依存の分裂機構の存在が明らかになってきている。収縮環非依存の分裂機構は、細胞性粘菌を用いた研究において初めて発見された。ミオシン重鎖欠損細胞は震盪培養では、ミオシンが欠損しているため、力発生ができない結果細胞質分裂ができず、多核・巨大化して、最終的に致死となる。しかし、このようにして多核・巨大化させたミオシン欠損細胞を基質上に接着させると、細胞の数箇所が別方向へ動き始め、最終的に幾つかの細胞に分裂する。この細胞質分裂は細胞周期に無関係に行われる。この分裂機構は細胞先導端で発生する基質に対する牽引力により進行すると考えられ、traction-mediated cytofission と呼ばれている。一方、基質上で継代培養されたミオシン欠損細胞は細胞周期依存的に分裂する。この分裂は細胞周期をともなうので、traction-mediated cytofission とは異なる細胞質分裂機構と考えられている。したがって細胞質分裂機構には複数の様式があると考えられる。従来の収縮環依存の細胞質分裂を cytokinesis A、収縮環非依存で細胞周期と共役する細胞質分裂を cytokinesis B、収縮環非依存で細胞周期に共役しない細胞質分裂を cytokinesis C と名付けられてきて

いる。これまで、cytokinesis BおよびCの分子機構についてはよくわかっていない。

本研究では、ミオシン欠損細胞を用いてcytokinesis Bの分裂機構解明を目的として行った。この機構はアクチンとミオシンの相互作用で発生する力を必要としないので、基質に対するアクチン依存的な牽引力の発生により進行すると考えた。そこで、GFPアクチン-コンストラクトを形質導入したミオシン欠損粘菌細胞の細胞下底部におけるアクチンの動態をTIRF（total internal reflection fluorescence）顕微鏡により観察した。その結果、アクチンの巨大な動的構造が分裂期特異的に細胞核直下の細胞表層に出現することがわかった。本研究では、この新奇アクチン構造をMiDAS (mitosis-specific dynamic actin structure)と名づけ、この構造の形成機構と機能を調べた。MiDASは核分裂にともない分裂し、さらに細胞質分裂の進行につれて細胞両極に移動した。この移動軌跡は分裂時の核や中心体の動態に類似するとわかった。そこで、MiDAS形成は中心体から伸長する微小管により誘導されると考え、細胞下底部のアクチンと微小管の分布を比較した。mCherryアクチンとGFPαチューブリン-コンストラクトを共発現させたミオシン欠損分裂細胞をTIRF顕微鏡により観察すると、大部分の星状体微小管は分裂期を通じてMiDAS領域内の細胞下底部に接触していた。また、星状体微小管を微小管重合阻害剤であるチアベンダゾールにより破壊すると、細胞両極のMiDASは速やかに消失した。これらの結果より、MiDASの形成は星状体微小管を介する機構により誘導されると考えられる。MiDAS領域のGFPアクチンの蛍光退色実験とTIRF顕微鏡観察より、MiDASは多数の点状のアクチン構造により構成されていることがわかった。点状アクチンは位置を変えずに出現と消失を繰り返していた。したがって、MiDAS領域は点状アクチンの出現消失により、その分布を変えると示唆された。次に、MiDASの機能を調べた。約10%のミオシンII欠損細胞は基質上でも細胞質分裂は失敗する。この

とき MiDAS は分裂途中で消失するとわかった。また、チアベンダゾールにより人為的に MiDAS を消失させたときでも、ミオシンⅡ欠損細胞は分裂に失敗した。したがって、MiDAS は基質依存の細胞質分裂の進行に重要な構造といえる。IRM (Interference reflection microscopy)観察から、MiDAS 領域は基質に近接する構造とわかった。さらに、細胞体を水流により吹き飛ばすと、MiDAS 領域のみが基質に残存した。したがって、この構造は基質へ強く接着していることがわかった。以上から、MiDAS は基質に牽引力を伝える移動可能な足場として機能することで基質依存の分裂進行に重要な役割を果たすと示唆された。